IEEE Photonics Journal
An IEEE Photonics Society Publication

Open Access

Ultraviolet Electrostatic Field Effect Light-Emitting Diode

Volume 12, Number 5, October 2020

Matthew Hartensveld, *Student Member, IEEE*
Bryan Melanson
Jing Zhang, *Member, IEEE*

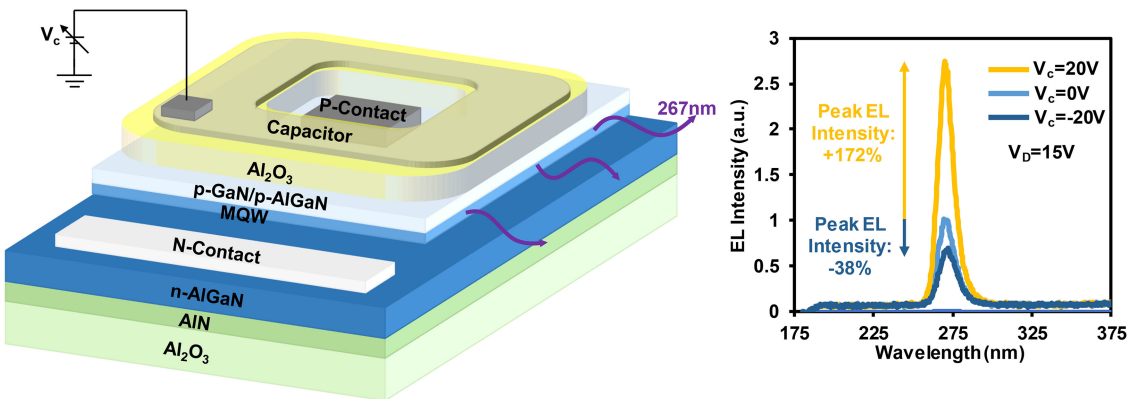

DOI: 10.1109/JPHOT.2020.3020384

Ultraviolet Electrostatic Field Effect Light-Emitting Diode

Matthew Hartensveld,[1] ***Student Member, IEEE***,
Bryan Melanson,[1] **and Jing Zhang**,[2] ***Member, IEEE***

[1]Microsystems Engineering Department, Rochester Institute of Technology, Rochester, NY 14623 USA
[2]Electrical and Microelectronic Engineering Department, Rochester Institute of Technology, Rochester, NY 14623 USA

DOI:10.1109/JPHOT.2020.3020384

Manuscript received August 10, 2020; accepted August 24, 2020. Date of publication August 31, 2020; date of current version September 14, 2020. This work was supported in part by the National Science Foundation under Award ECCS 1751675, and in part by the Office of Naval Research under Award N00014-16-1-2524. Corresponding authors: Matthew Hartensveld; Jing Zhang (e-mail: mth4891@rit.edu; jzeme@rit.edu).

Abstract: The potential of ultraviolet (UV) AlGaN quantum well (QW) light-emitting diodes (LEDs) is stunted due to the lack of efficient p-type doping for this ultra wide bandgap material. In this work, a novel device - UV electrostatic field effect LED (EFELED) is demonstrated to address this issue by significantly improving hole injection into the QW active region which leads to a relative increase of external quantum efficiency (EQE) up to 42%. The UV EFELED is realized by integrating a capacitor layer on top of a conventional 267 nm AlGaN QW LED, which introduces band bending to assist hole injection under a forward bias. A 10x increase in injection current is achieved through the application of a positive bias to the integrated capacitor layer. With 20 V applied to the capacitor, a 42% increase of EQE is achieved. Photon intensity modulation is demonstrated with the application of varying capacitor biases, which presents a novel brightness control at UV wavelength. Thus, the proposed UV EFELED provides significantly improved hole injection through a capacitor integration, which leads to high-efficiency UV LEDs for important applications such as sterilization and purification.

Index Terms: LED, GAN, FET, electrostatic doping, LED display, capacitor, LiFi.

1. Introduction

The AlGaN QW UV LEDs are being developed for applications such as virus sterilization, water purification, and medical treatments, as a replacement for mercury vapor lamps [1]–[4]. UV LEDs offer compact sizes, wavelength tuning, long lifetimes, and sustainability over mercury vapor lamps [1], [5]. Longer wavelength LEDs find widespread commercial use for lighting and display applications, highlighting the potential [5]–[7]. However, UV LEDs struggle with poor EQE of typically less than 10% for wavelengths below 300 nm [1]–[3]. A main factor limiting the efficiency is the poor p-type doping of the wide bandgap AlGaN. The ionization energy for the Mg p-type dopant depends on the Al-content from the AlGaN material, which ranges from that of GaN at 170 meV to that of AlN at $>$500 meV [8], [9]. With the large p-type ionization energy, far less than 1% of the p-dopant is ionized in AlGaN. Due to the lack of available holes, an imbalance with the abundant electrons exists which limits photon generation. The lack of conducting holes in the p-type layer also leads to high resistance and degrades device performance. Currently, there are two approaches to address

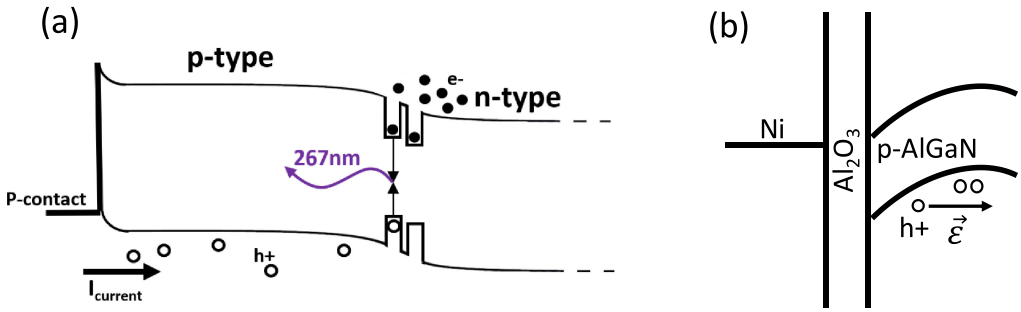

Fig. 1. (a) Forward biased LED showing steady state hole supply from the p-contact, (b) Positive bias to the Ni/Al_2O_3 capacitor causing energy band bending directing holes towards the MQW region.

this issue: use of a current spreading layer or use of polarization doping [10], [11]. Nevertheless, the use of a current spreading layer often leads to UV photon absorption issues, while the use of polarization doping requires precise control of epitaxial growth of graded AlGaN layers. In this paper, a third method is introduced which is by the use of energy band bending.

Energy band bending is already utilized in LED devices, where a positive voltage applied to the p-contact with respect to the n-contact lowers the built-in potential allowing current to flow, Fig. 1(a). A steady state current of holes is provided by the p-contact to resupply holes that recombine in a forward biased LED. The issue, however, is that the band bending in a forward biased LED is localized around the p-contact [10]. As the distance from the p-contact increases, the band bending is reduced, limiting the injection of holes to produce light in these regions. The metal p-contact area cannot span the entire p-type region due to significant absorption issues, which degrades light extraction efficiency (LEE). Thinner, optically transparent, conductors are commonly employed such as thin metal films, however, these thin films suffer from high resistance [12]. In order to apply additional band bending and to better utilize available holes, a capacitor is chosen while the p-contact still acts as the steady state source of holes.

Previous work has investigated the capacitor integration with InGaN/GaN visible LEDs showing EQE enhancements of 115%, this work is expanded upon here for UV LEDs [13]. Novel to this work, the capacitor is integrated with the AlGaN material system, forming a UV EFELED. The operation of the capacitor is analogous to that of the gate in a field effect transistor (FET), where charges can be attracted or repelled [14], [15]. The width of the depletion region (W) where charges are attached or repelled can be found through Eq. 1, where ε_s is the permittivity of the semiconductor, $\emptyset_{Fp}$ is the surface potential, V_a is the applied bias, q is the electron charge, and N_a is the p-type doping [16]. A thin layer of Ni is utilized as the optically transparent top plate of the capacitor, while a layer of Al_2O_3 is utilized as the dielectric, as shown in Fig. 1(b). The capacitor eliminates the resistance issue for thin metal current spreading layers, as virtually no current flows through the capacitor, and instead charges build up. Additionally, the Al_2O_3 thin film can serve to passivate surface states and enhance the LEE of the LED [17]. The performance increases by the UV EFELED are achieved by applying a positive bias to the capacitor in order to order to bend the bands further from the p-contact, repelling holes from the surface towards the multiple quantum well (MQW) region to recombine, as shown in Fig. 1(b).

$$W = x_{dT} = \sqrt{\frac{4\varepsilon_s \emptyset_{Fp} - V_a}{qN_a}} \tag{1}$$

Eq. 1. Width of the depletion region for a capacitor on a p-type semiconductor.

Holes are located uniformly throughout the p-type layer, though as previously mentioned, only the holes around the p-contact experience conduction due to the band banding and electric field created by the p-contact, Fig. 2(a). Holes located further away from the p-contact are unable to contribute to the current flow. At an initial time, with the application of a positive bias to the capacitor, in addition to the p-contact, the energy bands further from the p-contact also bend, directing holes

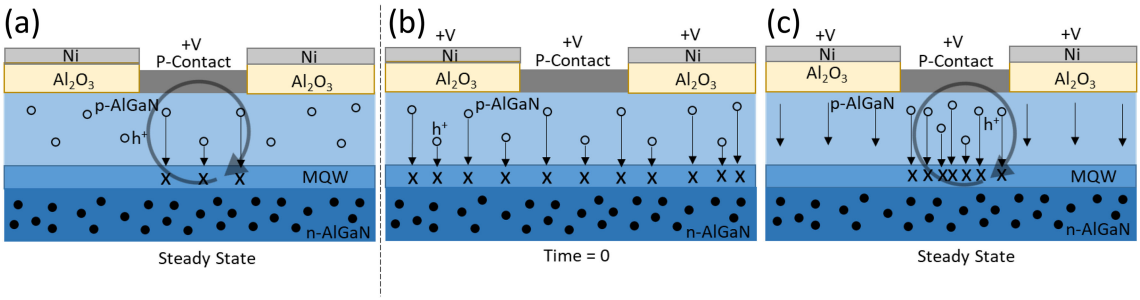

Fig. 2. (a) Positively biased p-contact under steady state showing path of holes, (b) positively biased p-contact and capacitor at initial time, and (c) positively biased p-contact and capacitor under steady state showing path of holes.

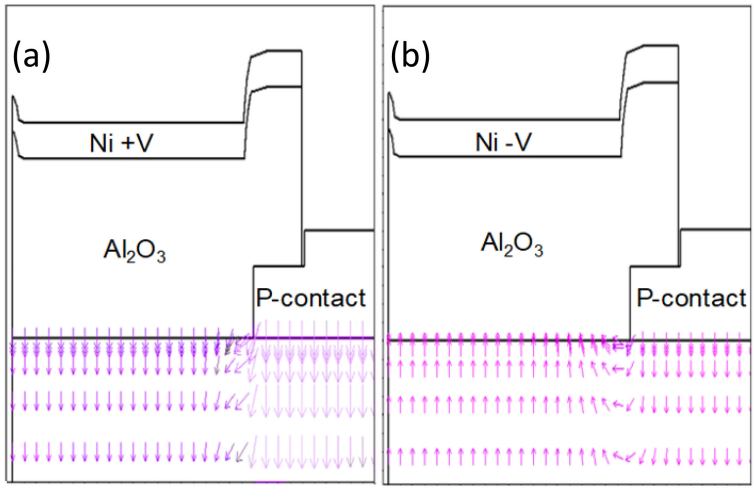

Fig. 3. UV EFELED Silvaco Atlas simulated electric field showing (a) positive biased capacitor, (b) negatively biased capacitor. Both with positively biased p-contact.

to the MQW region, as shown in Fig. 1(b) and Fig. 2(b). These holes modulated by the capacitor similarly recombine with electrons in the MQW region, as is the case with those from the p-contact. Due to charge neutrality, these holes that recombine either radiatively or non-radiatively must be resupplied. The p-contact, as is the case in conventional LEDs, is the steady and continuous source for holes, Fig. 2(c). The holes must be resupplied by the p-contact as the capacitor has negligible leakage current. Effectively in steady state, the areas under the capacitor become depleted, while the area under the p-contact gains these holes. These additional holes under the p-contact produce a highly conductive pathway and greatly enhance photon generation. Therefore, both the internal quantum efficiency (IQE) and EQE are greatly enhanced by this novel method.

A secondary benefit of utilizing a capacitor to cause band bending, is the additional hole ionization through Frankel-Poole field ionization [18]–[21]. Due to the additional energy band bending, the barrier to hole ionization is lowered, allowing for added holes to participate in conduction, which further increases photon emission [18]–[21]. The electric field lines formed by the capacitor are shown in Fig. 3(a) through Silvaco Atlas simulations.

In contrast to the enhancement in EQE by forward biasing the capacitor, the opposite effect can occur in the case of a reverse capacitor bias. If a negative voltage is applied instead to the capacitor plate, the barrier for holes is raised which causes the electric field lines to point towards the surface, as shown in Fig. 3(b). Holes are then trapped at the surface in order to compensate for the negative charge placed on the metal plate of the capacitor. Most of the trapped holes are from areas away from the p-contact which would normally not participate in conduction. However, some holes near

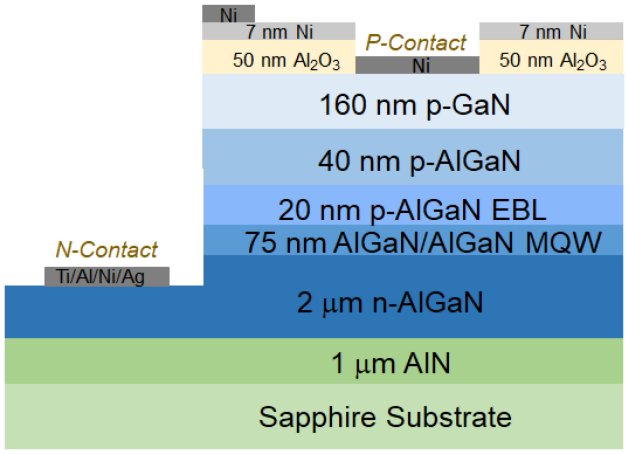

Fig. 4. Schematic cross section of fabricated UV EFELED device.

the edges of the p-contact are affected and instead of recombining in the MQW, are instead pulled to the capacitor, as shown by Fig. 3(b). With a negative bias applied to the capacitor, the EQE is reduced, though the reduction is comparatively small. The EQE drop is smaller than the EQE gain due to most of the holes that are captured not normally participating in conduction. Both the EQE gain during a positive capacitor bias, and a drop during a negative bias, are increased with higher LED forward biases due to the greater demand for holes.

These devices are realized with conventional AlGaN UV LEDs and are both electrically and optically tested. Four different capacitor designs are studied in order to best optimize the UV EFELED. This work opens the door to greatly improving the performance of UV LEDs and the potential UV applications.

2. Device Fabrication

The AlGaN UV LEDs emitting at 267 nm are grown through metal organic chemical vapor deposition (MOCVD) on a sapphire substrate. A 1 μm AlN buffer layer is grown on the sapphire, followed by 2 μm of n-AlGaN, 75 nm of AlGaN-AlGaN MQWs, 20 nm of p-AlGaN as an electron blocking layer, 40nm of p-AlGaN, and then 160nm of p-GaN. The mesa region is formed through the use of a chlorine plasma in a Lam 4600 reactive ion etcher with a photoresist hard mask. A 25/150/30/50 nm stack of Ti/Al/Ni/Ag was lifted off to form a common n-metal contact across the device. A 50 nm layer of Al_2O_3 was next deposited through atomic layer deposition (ALD) to form the dielectric for the capacitor. A 7 nm film of Ni was deposited and lifted off to act as the transparent top plate for the capacitor. The thin Ni film was also utilized as the hard mask with buffered oxide etch (BOE) to etch away the Al_2O_3 on the surface, leaving the film solely under the top capacitor plate. As a final step, a 50 nm coating of Ni was deposited to form both the p-contact and a thicker metal pad to probe the capacitor plate. No annealing step was performed for the metal contacts. Integration of the capacitor only required the addition of one masking level to a conventional LED, or the same in the case of a current spreading LED. A schematic view of the fabricated device can be seen in Fig. 4.

Four separate capacitor and p-contact designs were fabricated in order to optimize device performance. These designs are shown in Figs. 5(a–d) with an edge capacitor (design A), capacitor surrounding the central contact (design B), capacitor block with bar contact (design C), and capacitor block with edge contact (design D), respectively. These LED designs were fabricated to be 100 μm^2 in size. The devices had a contact area of 10 μm^2 for the p-contact and the capacitor, except for deign C with a contact area of 10 μm $\times$ 60 μm.

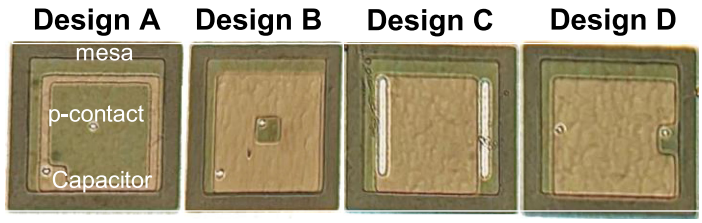

Fig. 5. UV EFELED fabricated designs (A-D) with differing capacitor and p-contact arrangements.

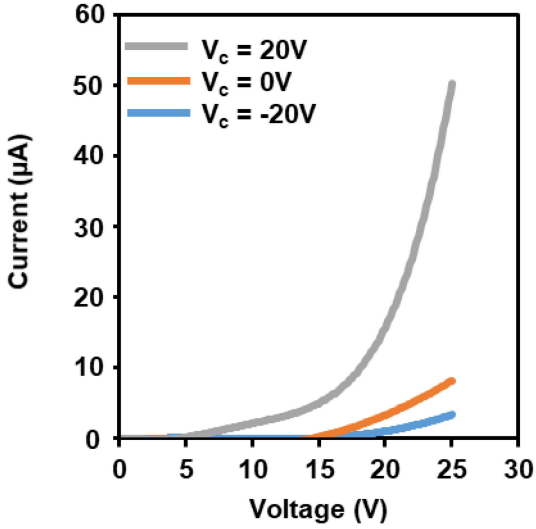

Fig. 6. I-V curves from the UV EFELED with design C showing the I-V performance.

3. Results and Discussion

Both electric and optical measurements were performed on the fabricated UV EFELED devices in order to explore the physics of band bending and the effect on hole injection. The integrated capacitor is biased independently in this design to allow for separate modulation apart from driving the LED. The capacitor contact can be shorted to the p-contact if the goal is a pure performance gain, separate from the novel ability to modulate photon generation.

The I-V characteristics were collected, with capacitor voltages varying from 20 V to −20 V, while the UV LED was driven at a forward voltage from 0 to 25 V. As a representative example, I-V results of design C are shown in Fig. 6. From Fig 6, it can be seen that the application of a positive capacitor bias is seen to drastically increase the drive current by ∼10x due to the utilization of additional holes. The increased hole concentration below the p-contact forms a far more conductive pathway for current transport. Under positive capacitor bias, Fig. 6 further shows the increased conduction leads to a lower turn-on voltage for the LED due to the greater hole concentration lowering the Schottky barrier formed by the p-contact. Capacitor leakage was recorded on average to be 9 pA from the tested capacitor voltages. This shows the drive current enhancement is due to the added band bending and not capacitor leakage. Opposite performance is seen in the case of a negative capacitor bias, with a reduction in the drive current of ∼60%, Fig 6. The diode also has a higher turn-on voltage due to a fraction of the holes captured instead of participating in conduction.

Each of the tested capacitor designs showed a similar trend of enhancement with a positive capacitor bias and a decrease with a negative bias. In order to compare the four designs to best optimize the device performance, the I-V curves of each are recorded in Fig. 7. Here each capacitor voltage is held at 20 V to compare the current enhancement. It is clear that as the capacitor size increases the enhancement in drive current is greatly improved. Position and size of the p-contact

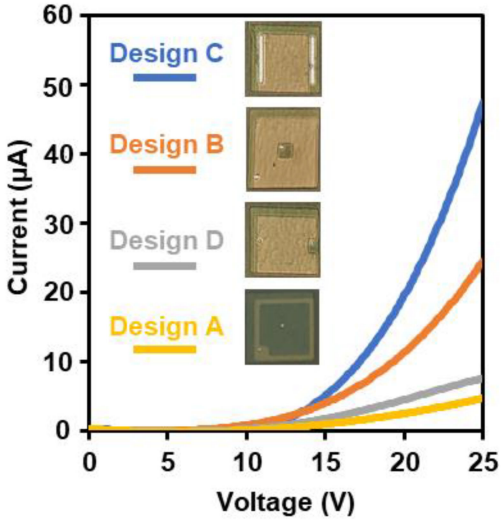

Fig. 7. I-V curves with designs (A-E) held at a capacitor voltage of 20 V.

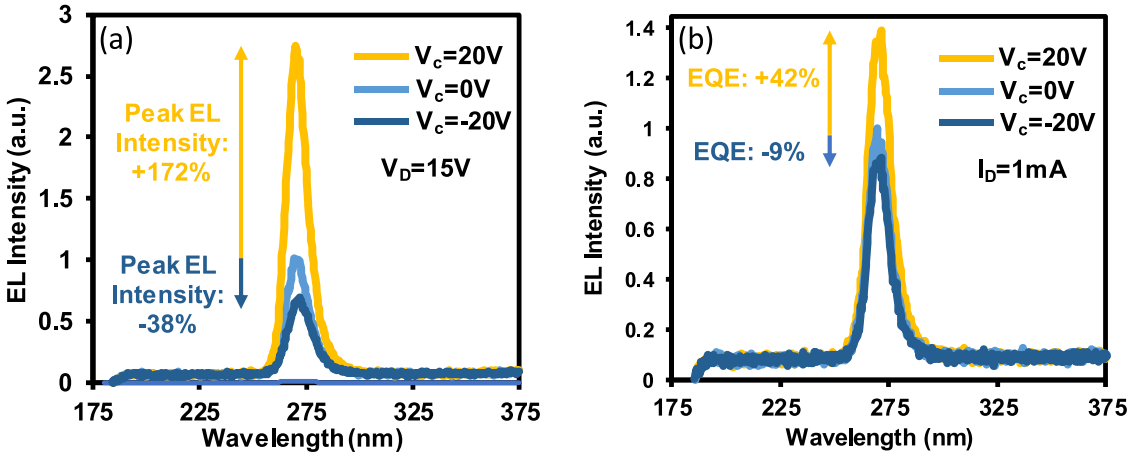

Fig. 8. (a) Measured EL intensity for with varying capacitor biases at a forward voltage of 15 V, (b) measured EL intensity with varying capacitor biases at a constant current of 1 mA.

are also important to the UV EFELED device efficiency. Location of the p-contact on the edge, as is the case of design D, leads to a lower drive current than design B for a similar capacitor area. Position of the contact near the edge can lead to surface recombination that can degrade current flow. Design C shows that a further gain in drive current is obtained by increasing the p-contact length from 10 μm to 60 μm. For larger p-contact sizes, the injected holes are not as confined and are able to better spread across the device, leading to lowered resistance. However, a larger p-contact leads to significant photon absorption. A future optimized design would call for a large capacitor with a thin p-contact metal in the middle that spans across the device, such as a star shaped contact with a surrounding capacitor.

Optical measurements through electroluminescence (EL) were taken in order to judge the optical performance of the device. The EL spectra are plotted in Fig. 8 for design C. Design C is selected as it was seen to have the best performance enhancement, seen by Fig. 7. To compare the peak EL intensity, Fig. 8(a), the capacitor is varied from 20 V to -20 V, while holding the drive voltage (V_D) constant at 15 V. With the application of 20 V to the capacitor the peak EL intensity is increased by 172%. The additional holes involved in conduction, which are the main limitation in UV LEDs,

generates greater recombination with the plentiful electrons. In contrast, −20 V to the capacitor produces a decrease in peak EL intensity by 38% due to the captured holes from the capacitor.

In order to compare the EQE of the UV EFELED, EL measurements are taken at a constant current of 1 mA. The corresponding EL spectra are recorded in Fig. 8(b) with the capacitor varied from 20 V to −20 V. The 1 mA is the total current to the whole device, including the capacitor, though the capacitor shows pA of leakage current. To extract the EQE, the integral of the curves are taken for each tested capacitor bias. At 20 V applied to the capacitor the relative EQE is seen to be dramatically increased by 42%, which greatly helps the commercial viability of UV LEDs. Applying −20 V to the capacitor leads to the opposite of a slight decrease in the relative EQE of 9%. Increased positive or negative biases are expected to have a larger impact on EQE until the capacitor breaks down. Modulation of photon emission through the independent bias of the capacitor, presents a novel way to control the brightness of UV LEDs.

4. Conclusion

The work presented here introduces a capacitor-UV LED integration, known as a UV EFELED. The major limit of UV LEDs, the lack of p-type doping, is addressed through a novel solution. The UV EFELED makes use of an Al_2O_3 dielectric and thin transparent Ni film to form a capacitor on top of the p-type layer. An additional electrostatic field is produced by the capacitor in order to drive holes towards to the MQW to recombine and be recycled. Due to the capacitor with hole modulation, positive voltages lead to an increase in photon production and efficiency. The EQE was increased by a record 42% due to the capacitor integration. Capacitor integration also produces a novel means of brightness control with positive biases increasing photon generation, while negative biases limit generation through hole reduction. The fabrication of the UV EFELED is compatible with most conventional UV LED processes, requiring only one additional mask level. Thus, this work shows immense promise to address the limiting issue of poor p-type doping for AlGaN and therefore further the market viability.

References

[1] M. Kneissl and J. Rass, "A brief review of III-Nitride UV emitter technologies and their applications," *III-Nitride Ultraviolet Emitters: Technology and Applications*. 1st ed., New York, NY, USA: Springer, 2016, ch. 1, pp. 1–25.
[2] H. Hirayama, N. Maeda, S. Fujikawa, S. Toyoda, and N. Kamata, "Recent progress and future prospects of AlGaN-based high-efficiency deep-ultraviolet light-emitting diodes," *Japanese J. Appl. Phys.*, vol. 53, no. 10, 2014, Art. no. 100209.
[3] S. Lee, H. Kim, M. Choi, and K. Byun, "New design and application of high efficiency LED driving system for RGB-LED backlight in LCD display," in *Proc. IEEE Power Electron. Specialists Conf.*, 2006, pp. 1–5.
[4] P. Jarvis, O. Autin, E. Goslan, and F. Hassard, "Application of ultraviolet light-emitting diodes (UV-LED) to full-scale drinking-water disinfection," *Water*, vol. 11, no. 9, 2019, Art. no. 1894.
[5] S. Nakamura and M. Krames, "History of gallium–nitride-based light-emitting diodes for illumination," *Proc. of the IEEE*, vol. 101, no. 10, pp. 2211–2220, Oct. 2013.
[6] T. Tsunemasa, "Present status of energy saving technologies and future prospect in white LED lighing," *IEEJ Trans.*, vol. 3, pp. 21–26, 2008.
[7] F. Li, D. Chen, X. Song, and Y. Chen, "LEDs: A promising energy-saving light source for road lighting," in *Proc. IEEE PES Asia-Pacific*, 2009, pp. 1–3.
[8] W. Götz, M. Johnson, J. Walker, D. P. Bour, and R. A. Street, "Activation of acceptors in Mg-doped GaN grown by metalorganic chemical vapor deposition," *Appl. Phys. Lett.*, vol. 65, no. 5, 1996, Art. no. 667.
[9] Y. Taniyasu, M. Kasu, and T. Makimoto, "An aluminium nitride light-emitting diode with a wavelength of 210 nanometres," *Nature*, vol. 441, no. 7091, pp. 325–328, 2006.
[10] B. Cao *et al.*, "Effects of current crowding on light extraction efficiency of conventional GaN-based light-emitting diodes," *Opt. Express*, vol. 21, no. 21, 2013, Art. no. 25381.
[11] J. Simon, V. Protasenko, C. Lian, H. Xing, and D. Jena, "Polarization-induced hole doping in wide-band-gap uniaxial semiconductor heterostructures," *Science*, vol. 327, no. 5961, pp. 60–64, 2009.
[12] F. Lacy, "Developing a theoretical relationship between electrical resistivity, temperature, and film thickness for conductors," *Nanoscale Res. Lett.*, vol. 6, no. 1, 2011, Art. no. 636.
[13] M. Hartensveld, B. Melanson, and J. Zhang, "Electrostatic field effect light-emitting diode," *IEEE Photon. J.*, vol. 12, no. 3, Jun. 2020, Art. no. 8200408.
[14] G. Gupta, B. Rajasekharan, and R. Hueting, "Electrostatic doping in semiconductor devices," *IEEE Trans. Electron Devices*, vol. 64, no. 8, pp. 3044–3055, Aug. 2017.

[15] H. Sood, V. Srivastava, and G. Singh, "Advanced MOSFET technologies for next generation communication systems - perspective and challenges: A review," *J. Eng. Sci. Techn. Rev.*, vol. 11, no. 3, pp. 180–195, 2018.
[16] C. Hu, "PN and metal-semiconductor junctions," *Modern Semiconductor Devices for Integrated Circuits*, 1st ed., Pearson, 2009, ch. 4, pp. 89–156.
[17] M. Pawlik *et al.*, "Electrical and chemical studies on Al_2O_3 passivation activation process," *Energy Procedia*, vol. 60, pp. 85–89, 2014..
[18] J. Simmons, "Poole-Frenkel effect and schottky effect in metal-insulator-metal systems," *Physical Rev.*, vol. 155, no. 3, pp. 657–660, 1967.
[19] P. Kozodoy, M. Hansen, S. DenBaars, and U. Mishra, "Enhanced Mg doping efficiency in Al0.2Ga0.8N/GaN superlattices," *Appl. Phys. Lett.*, vol. 74, no. 24, pp. 3681–3683, 1999.
[20] E. Schubert, W. Grieshaber, and I. Goepfert, "Enhancement of deep acceptor activation in semiconductors by superlattice doping," *Appl. Phys. Lett.*, vol. 69, no. 24, pp. 3737–3739, 1996.
[21] J. Jamaux, "Polarization-induced doping and its application to light-emitting diodes," M.S. thesis, Dept. Mater. Eng., McGill Univ., Canada, 2014.